J ENDOVASC THER
2009;16:531–538

◆ EXPERIMENTAL INVESTIGATION ◆

In Vivo Deformation of the Human Abdominal Aorta and Common Iliac Arteries With Hip and Knee Flexion: Implications for the Design of Stent-Grafts

Gilwoo Choi, MS[1]; Lewis K. Shin, MD[2]; Charles A. Taylor, PhD[1,3,4]; and Christopher P. Cheng, PhD[4]

Departments of [1]Mechanical Engineering, [3]Bioengineering, and [4]Surgery, Stanford University, Stanford, California, USA. [2]Department of Radiology, Stanford University/VAPAHCS, Stanford, California, USA.

Purpose: To quantify in vivo deformations of the abdominal aorta and common iliac arteries (CIAs) caused by musculoskeletal motion.
Methods: Seven healthy subjects (age 34±11 years, range 24–50) were imaged in the supine and fetal positions (hip flexion angle 134.0°±9.7°) using contrast-enhanced magnetic resonance angiography. Longitudinal strain, twisting, and curvature change of the infrarenal aorta and CIAs were computed. The angle between the left and right CIAs and translation of the arteries were also computed.
Results: Maximal hip flexion induced shortening (5.2%±4.6%), twisting (0.45±0.27 °/mm), and curvature changes (0.015±0.007 mm^{-1}) of the CIAs. The angle between the CIAs increased by 17.6°±8.6°. The iliac arteries moved predominantly in the superior direction relative to the aortic bifurcation, which would induce compression and bending, thus increasing curvature and angle between the CIAs. The abdominal aorta also exhibited shortening (2.9%±2.1%) and twisting (0.07±0.05 °/mm) deformation associated with the hip flexion.
Conclusion: Although this study was limited to a few healthy young adults, musculoskeletal motion, specifically hip flexion, caused significant in vivo morphological changes (shortening, twisting, and bending) of the arteries. Predominant superior translation of the CIAs was observed, which suggests that preclinical testing of cyclic superior-inferior translational motion may aid in predicting stent-graft fractures. In turn, stent-graft design could be improved, decreasing overall stent-graft–related complications.
J Endovasc Ther. 2009;16:531–538

Key words: abdominal aorta, common iliac artery, in vivo study, deformation, strain, curvature, twisting

Endovascular aneurysm repair (EVAR), compared to open surgical repair, has been increasingly utilized due to faster patient recovery, reduced morbidity and mortality, and minimal invasiveness for high-risk patients.[1–5] However, metallic stent fracture (9%),[6,7] modular component separation (13%),[8] and stent migration (8%)[9] have been

Funding for this study was provided by the National Institutes of Health (NIH; P41 RR09784, U54 GM072970) and the National Science Foundation (0205741). In accordance with the NIH Public Access Policy, this article is available for open access at PubMed Central.

The authors have no commercial, proprietary, or financial interest in any products or companies described in this article.

Address for correspondence and reprints: Gilwoo Choi, James H. Clark Center, Room E350, 318 Campus Drive, Stanford, CA 94305-5431 USA. E-mail: *giroo@stanford.edu*

reported as common failure modes that may result in serious clinical complications such as endoleak and rupture.[10,11]

Although government regulators have made significant efforts to improve preclinical evaluation of endovascular grafts, current testing protocols have not successfully predicted the aforementioned failure modes.[12,13] For designing preclinical tests, cardiac pulsation and respiratory motion have been the primary loading considerations in the form of pulsatile fatigue testing. On the other hand, static characteristics of the abdominal aorta, including the size and shape of the aortic neck, bifurcation divider offset, branch angle, and angular asymmetry, have been extensively investigated, since the geometry of the aorta is crucial for designing and implanting endovascular devices.[14–16]

In our view, however, one of the recognized problems with current device evaluation has been the lack of information about ''dynamic'' and ''non-pulsatile'' in vivo deformations of the vessels. Anatomically, the common iliac arteries (CIAs), where the limb components of the stent-graft land, are in proximity of the hip joint. Thus, the abdominal aorta and the CIAs are subjected to dynamic forces that the musculoskeletal system may induce during hip flexion. If such forces act on the vessels repeatedly, the integrity of endovascular devices may be significantly compromised. We believe a better understanding of these vessel deformations due to musculoskeletal motions would improve both device development and clinical decision making.

In this study, we utilized magnetic resonance angiography (MRA) and image processing methods to quantify 3-dimensional (3D) in vivo deformation of the abdominal aorta and CIAs by maximal hip flexion. Measurements of longitudinal, twisting, and curvature deformations, as well as changes in angle between left and right CIAs, may enable the development of more reliable preclinical tests.

METHODS

Imaging Protocol and Study Population

The abdominal aorta and CIAs of 7 healthy subjects (6 women; age 34±11 years, height 160±8 cm, weight 54±8 kg) were imaged using contrast-enhanced MRA in a clinical magnet (1.5-T Signa whole-body MR system; GE Medical Systems, Milwaukee, WI, USA). Each subject was imaged in the supine and fetal positions (hip flexion angle 134.0°±9.7°) to induce arterial deformation (Fig. 1). Ten mL of MultiHance gadolinium (Bracco Diagnostics, Inc., Milan, Italy) was administered via the left antecubital vein at 3 mL/s, followed by 10 mL of normal saline at 3 mL/s for each body position. Each scan lasted ~30 seconds and was performed during a breath hold to eliminate respiratory motion. The field of view was approximately 30×30×10 cm, with a reconstructed matrix size of 512×512×72. This study was approved by the Human Subjects Research Institutional Review Board, and informed written consent was obtained from each volunteer.

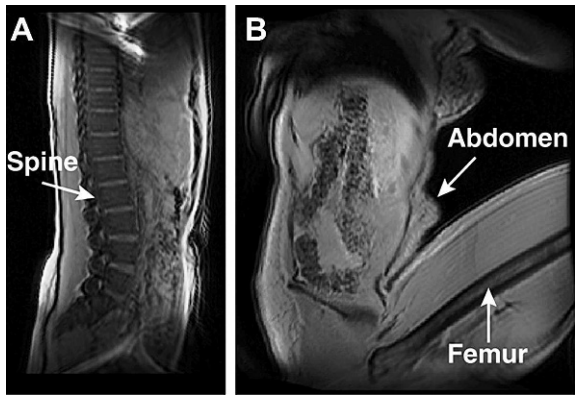

Figure 1 ◆ Sagittal views of a subject in the (**A**) supine and (**B**) fetal positions are displayed with the localizer scan images prior to MRA.

Image-Based Anatomical Modeling

Prior to image processing, geometric distortion of the MRA data caused by the inherent inhomogeneities in the magnetic field was corrected using proprietary software (GE Medical Systems).[17] Geometric changes in the vessel were then quantified by means of custom software (*www.simvascular.org*) and methods that we previously described.[18] A 2D threshold segmentation technique was used to find the lumen boundaries of the arteries (Fig. 2A). Fourier smoothing was then performed on the centroid sets of the segmentations to create a centerline.

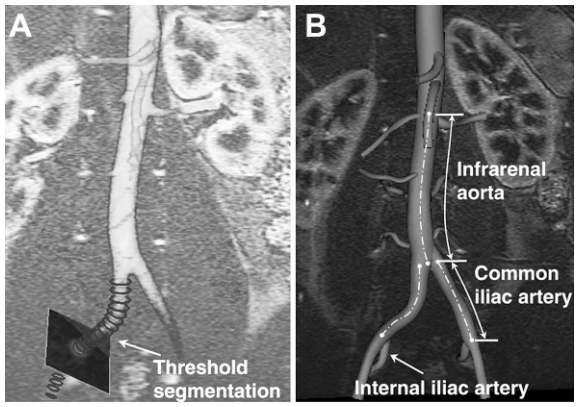

Figure 2 ◆ (**A**) Centerline path is generated by calculation of the centroids of the 2D threshold segmentations. (**B**) Ostia of the renal and internal iliac arteries and the aortic bifurcation are used as fiducial landmarks for analysis.

The smoothed centerline path was utilized in the calculation of longitudinal strain, axial twisting, and curvature metrics.

Deformation Metrics

To determine the strain, 2 measurements of the length changes in the infrarenal aorta were made using both renal arteries as reference points (Fig. 2B) since the offset distance (3.4 ± 0.9 mm) between the left and right renal arteries was relatively small ($3.7\% \pm 0.9\%$) compared to the total length of the infrarenal aorta. For the strain calculation in the CIAs, the internal iliac artery and the aortic bifurcation were used as landmarks. In addition, twisting deformation of the abdominal aorta was also measured by comparison of the angle of separation between a renal artery and a CIA (Fig. 3).[18] For the CIA, the aortic bifurcation and the ostium of the internal iliac artery were used to compute the angle of separation.[18]

To measure 10 angles between the left and right CIAs, 10 points were sampled in 5-mm increments along the artery from the starting point to a distal point on the iliac artery centerline (Fig. 4). Curvature of the aorta and CIA was calculated by the inverse of the radius of a circumscribed circle along the vessel.[18] Changes in mean curvature were then calculated between the supine and fetal positions; the maximum curvature for each position was also determined. In order to compare local

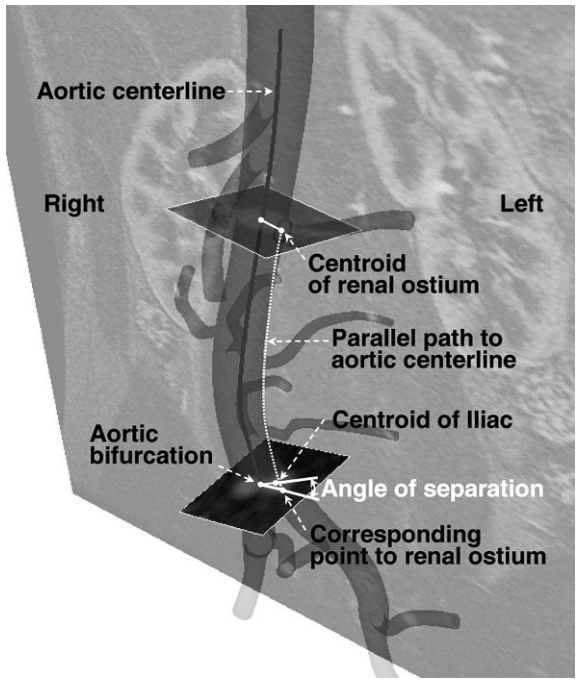

Figure 3 ◆ The method of calculating the angle of separation between the left renal and left CIAs. A parallel path to the aortic centerline, starting from the renal ostia centroid, is generated to find the corresponding point at the level of the aortic bifurcation. The angle of separation is determined by the corresponding point to the left renal ostium at the level of aortic bifurcation, aortic bifurcation point, and centroid of the left iliac lumen cross section.

curvature, the vessel was divided into segment lengths equal to the vessel radius, and curvature values were compared between the supine and fetal positions.

To investigate the kinematic cause of the observed arterial deformations, 2 geometries were co-registered based on the local geometry around the aortic bifurcation (Fig. 5). Although the abdominal aorta essentially undergoes non-rigid body deformation due to musculoskeletal motion, the CIAs can be co-registered on the basis of the local region at the aortic bifurcation. Thus, the co-registered geometries made it possible to track the relative motion of the artery with respect to the local region of the abdominal aorta. Specifically, since the coordinate system of image volumes for supine and fetal positions differs, the aortic bifurcation was employed as the origin of each local coordinate system.

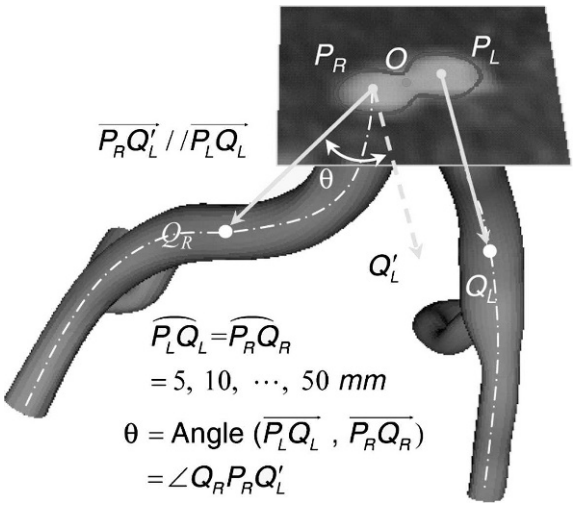

Figure 4 ◆ The intersection between the CIA centerline and the plane at the aortic bifurcation (O) defines the starting points of the CIAs, denoted as P_L and P_R. The angle between the left and right CIAs is determined by use of CIA vectors, defined from the starting points (P_L and P_R) to a distal point on the CIA centerline in 5-mm increments. Ten pairs of aortic bifurcation angles are compared between the supine and fetal positions.

An anterioposterior (AP) unit vector was defined by performing the cross product of the right-left (RL) and superior-inferior (SI) unit vectors. The SI unit vector (N_z) extended from the aortic bifurcation to a point 7 mm (approximate radius of the aorta) superior to the bifurcation; the RL unit vector (N_x) was defined from the left CIA centroid to the right CIA centroid at the level of the aortic bifurcation. On the basis of the orthogonal unit vectors defined, coordinate transformation was performed from the fetal (${}^F\vec{q}$) to supine (${}^S\vec{q}$) coordinate system as follows:

$$ {}^S\vec{q} = {}^SR_F({}^F\vec{q} - {}^F\vec{o}) + {}^S\vec{O}, \qquad (1) $$

where ${}^SR_F$ represents a rotation matrix, while ${}^F\vec{o}$ and ${}^S\vec{O}$ represent the coordinates of the aortic bifurcation in the fetal position coordinate system and in the supine coordinate system, respectively.

Statistical Analysis

All the deformation measurements are provided as means ± standard deviation. Each deformation metric for the supine and fetal positions was compared using paired and 2-tailed Student *t* tests to identify statistical significance ($p<0.05$). Analyses were performed using Matlab software (The MathWorks, Inc, Natick, MA, USA).

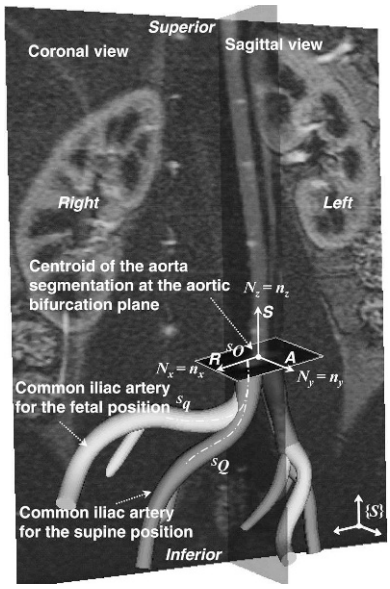

Figure 5 ◆ The common iliac artery for the fetal position (light grey) is co-registered with that for the supine position (dark grey) in the same coordinate system (S). Three orthogonal unit vectors in right-left, superior-inferior, and AP directions are used as reference vectors for co-registration. Note that the CIA exhibits significant translation-inducing morphological changes from the supine to fetal positions.

RESULTS

Deformation of the Abdominal Aorta

From the supine to fetal positions, the infrarenal aorta shortened 2.9%±2.1% (supine 92.0±6.8 mm, fetal 89.3±6.3 mm; $p<0.05$), and the mean curvatures of the abdominal aorta for the supine and fetal positions were not statistically different (supine 0.007± 0.002 mm^{-1}, fetal 0.008±0.004 mm^{-1}). Twisting of the abdominal aorta was $-3^\circ\pm7^\circ$ (p=NS) over the infrarenal aorta, where the negative sign represents a clockwise direction as viewed from the top of the abdominal aorta. The average magnitude, i.e., absolute value of the twisting angle, was $6^\circ\pm4^\circ$ ($p<0.05$). Accordingly, the twist rate was 0.07±0.05 °/mm.

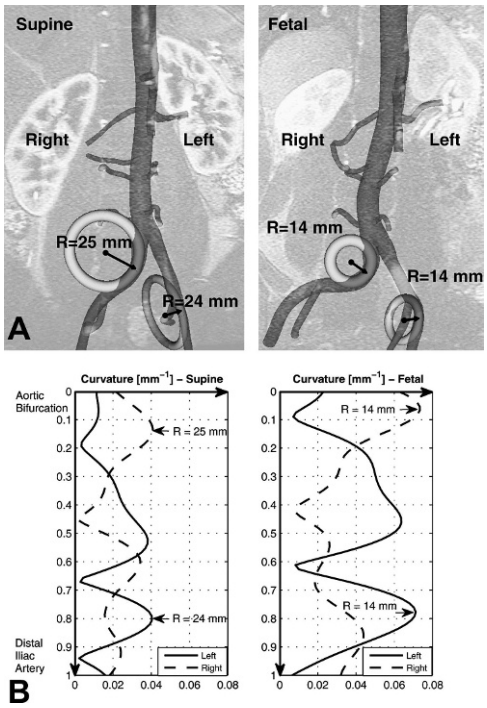

Figure 6 ◆ (**A**) Circles with radius of curvature at the maximum curvature for the supine and fetal positions are superimposed with geometric models for geometric interpretation. (**B**) Curvature variation of the iliac artery is plotted along the arc length of the iliac artery from the aortic bifurcation to distal iliac artery. Maximum curvature and corresponding minimum radius of curvature are denoted by arrows.

Deformation of the CIA

From the supine to fetal positions, the CIA segment shortened 5.2%±4.6% (supine 44.8±12.7 mm, fetal 42.6±12.5 mm; $p<0.05$) and twisted 18°±10° in magnitude ($p<0.05$). The corresponding twist rate was 0.45±0.27 °/mm. Mean curvature of the CIA increased 0.015±0.007 mm^{-1} (supine 0.019±0.006 mm^{-1}, fetal 0.034±0.010 mm^{-1}; $p<0.001$), which corresponded to an 85%±44% increase. Accordingly, the mean radius of curvature decreased 46%±21% (supine 100±52 mm, fetal 48±16 mm). The maximum curvature for the supine position was 0.038±0.013 mm^{-1}, while that for the fetal position was as high as 0.069±0.022 mm^{-1}. The corresponding minimum radius of curvature for the supine position was 29±12 mm, whereas that for the fetal position was 17±7 mm.

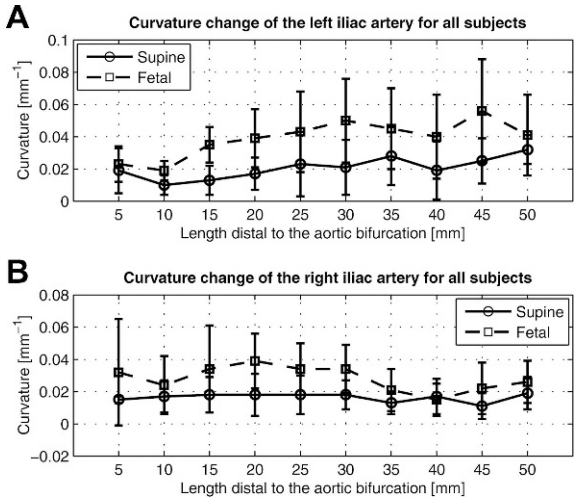

Figure 7 ◆ Curvature variation of the CIA for all subjects is plotted along 10 sampled locations of the artery (A: left iliac, B: right iliac). Total mean curvature increases from the supine to fetal position.

Figure 6 illustrates curvature variation along the arc length of the CIA and the geometric interpretation of the radius of curvature at the maximum curvature for both CIAs. In the left CIA, the radii of the circumscribed circles for the supine and fetal positions were 25 and 14 mm, respectively; in the right CIA, the radii were 24 and 14 mm, respectively. As shown in Figure 7, the local curvature exhibited non-uniform changes along the vessel length. At 30 mm distal to the aortic bifurcation, which is an average iliac fixation point,[19,20] the curvature for the left increased from 0.021±0.017 mm^{-1} to 0.050±0.026 mm^{-1}, while the curvature for the right increased from 0.018±0.009 mm^{-1} to 0.034±0.015 mm^{-1}. For the angle between the left and right CIAs, the farther the points moved distal to the aortic bifurcation, the more the angle increased due to joint flexion (Fig. 8). At 50 mm from the aortic bifurcation, the angle change was 17.6°±8.6° (supine 52.7°±7.1°, fetal 70.4°±13.9°).

CIA Translation

The co-registered geometries made it possible to quantify the translation of the CIAs due to hip flexion in 3 orthogonal directions (AP, RL, and SI). With regard to the translation in the AP and RL directions, the iliac arteries

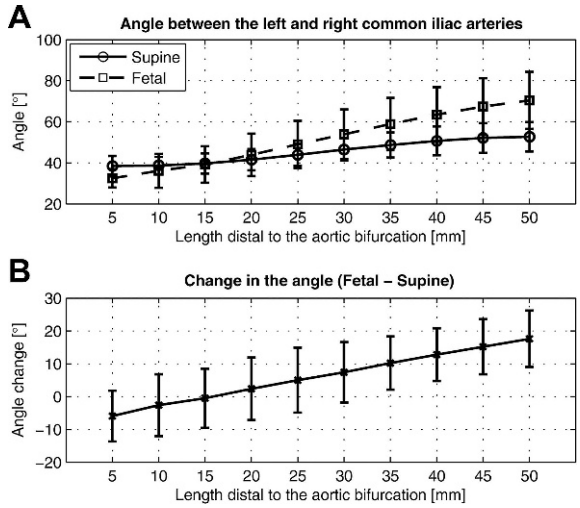

Figure 8 ◆ Angle between the left and right CIAs for each position is measured at 10 discretely sampled locations along the artery (**A**). From the supine to fetal positions, the angle between the left and right CIAs increases as more distal locations are compared (**B**).

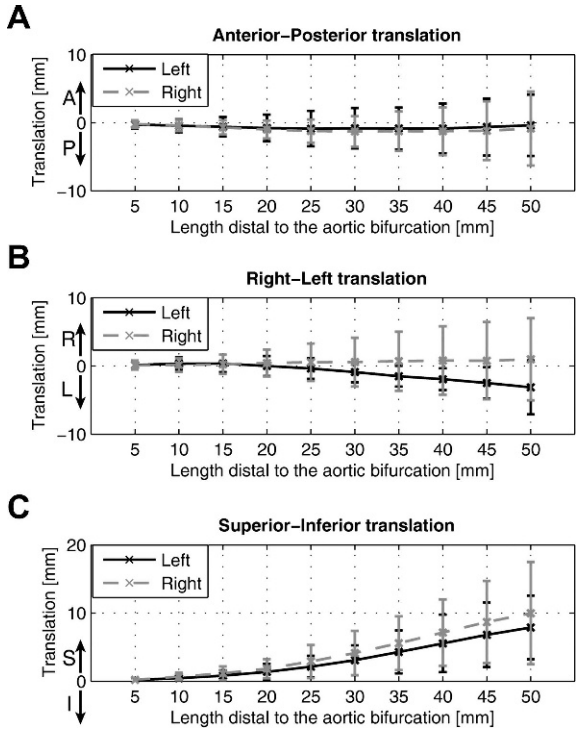

Figure 9 ◆ Translation of the CIA is plotted in anterior-posterior (AP), right-left (RL), and superior-inferior direction. Note that the superior translation is predominantly observed, as compared to AP and RL translations.

did not show significant motion (Fig. 9A,B). On the other hand, the predominant motion of the iliac arteries was, instead, in the superior direction due to maximal hip flexion (Fig. 9C). At 45 mm distal to the aortic bifurcation, which is an average iliac bifurcation point,[19] the left and right CIAs translated 6.8±4.7 mm and 8.7±6.0 mm in the superior direction, respectively.

DISCUSSION

This study provided new information on the in vivo non-pulsatile deformation of the abdominal aorta and iliac arteries caused by musculoskeletal motion. Furthermore, in vivo kinematics of the CIAs explained the observed deformations based on co-registration of the vessel geometry. Maximal hip flexion induced significant shortening, twisting, and bending of the CIAs. The abdominal aorta also exhibited shortening and twisting deformation from the supine to fetal positions. Abel et al.[12] suggested that durability tests and stress analyses for longitudinal and torsional loading and bending were some of the most critical areas needing improvement.

We found that the abdominal aorta shortened ~3% on average due to maximal hip flexion. The shortening may be attributed to hip flexion because the CIA was found to move superiorly with respect to the aortic bifurcation, compressing the distal abdominal aorta. Moreover, the abdominal aorta experienced ~6° twisting deformation, likely due to the asymmetric motion of the left and right CIAs, which could induce a torsional moment in the distal portion of the abdominal aorta. In this population, a consistent direction of twisting was not observed, probably due to individual anatomical variation, such as different branch bifurcation angles, or variable musculature lines of action.

Below the aortic bifurcation, the CIA shortened ~5% on average and twisted ~18° from the supine to fetal positions. In addition, mean curvature of the iliac artery for the fetal position increased ~85%, which corresponded to a ~46% decrease in radius of curvature. We also found that the change in the angle between the left and right CIAs increased almost linearly (R^2=0.99), progressing distal to the aortic

bifurcation. In other words, the iliac arteries curve away from each other, and thus the angle change is amplified moving distally.

These observed deformations, including significant shortening, curvature change, and angle change between the CIAs, probably result from the interaction between musculoskeletal and vascular systems in the lower extremities. Therefore, these deformations may predispose endografts to migration, resulting in type I and type III failures. The inability of an endograft to lengthen, shorten, or bend according to the changes in vessel length or curvature may impair fixation at the proximal and distal anchoring sites.

The co-registration of the CIAs revealed a predominant superior translation of the vessels relative to the aortic bifurcation, from the supine to fetal positions. Kinematically, the superior translation would induce longitudinal compression of the CIA with respect to the aortic bifurcation, causing shortening and bending of the artery, thus increasing curvature and angle between the CIAs.

Limitations

This study was limited to a few young, healthy volunteers who could fit in the magnet in the fetal position. For older or diseased subjects, the amount of vessel deformation may differ due to lengthening and stiffening.[21] There could be greater changes in curvature because displacements would have to be accommodated more by curving and less by shortening. However, we expect that vessel deformations in older subjects may exhibit similar trends because the kinematic motion of the lower extremities would be similar. In addition, the deformation measurements resulted from an extreme body position (fetal). Normal walking (mean hip flexion angle 43.2°)[22] would likely induce less deformation than maximal hip flexion (134.4°).

Conclusion

We have shown that the abdominal aorta and the CIAs readily conformed to musculoskeletal motion and exhibited significant deformations. Musculoskeletal motion, specifically hip flexion, caused significant in vivo morphological changes of the vessels, resulting in shortening, twisting, and bending of the abdominal aorta and the CIAs. Translation of the CIAs was predominantly in the superior direction, so pre-clinical testing of cyclic superior-inferior translational motion may aid in more reliable predictions of stent-graft durability. In turn, stent-graft design and manufacturing could be improved, decreasing overall stent-graft–related complications. Future studies will include analysis of vessel deformation in older and diseased subjects. Ultimately, investigation of in vivo deformations of actual stent-grafts will be required for more complete understanding of device failure mechanisms.

Acknowledgments: The authors gratefully acknowledge Anne M. Sawyer, Sandra Rodriguez, and Romi Samra for their assistance with the imaging studies at the Richard M. Lucas Center for Magnetic Resonance Imaging at Stanford.

REFERENCES

1. Adriaensen ME, Bosch JL, Halpern EF, et al. Elective endovascular versus open surgical repair of abdominal aortic aneurysms: systematic review of short-term results. *Radiology*. 2002;224:739–747.
2. Bolke E, Jehle PM, Storck M, et al. Endovascular stent-graft placement versus conventional open surgery in infrarenal aortic aneurysm: a prospective study on acute phase response and clinical outcome. *Clin Chim Acta*. 2001;314:203–207.
3. Cotroneo AR, Iezzi R, Giancristofaro D, et al. Endovascular abdominal aortic aneurysm repair: how many patients are eligible for endovascular repair? *Radiol Med*. 2006;111:597–606.
4. Parodi JC, Marin ML, Veith FJ. Transfemoral, endovascular stented graft repair of an abdominal aortic aneurysm. *Arch Surg*. 1995;130: 549–552.
5. Williamson WK, Nicoloff AD, Taylor LM, et al. Functional outcome after open repair of abdominal aortic aneurysm. *J Vasc Surg*. 2001; 33:913–920.
6. Jacobs TS, Won J, Gravereaux EC, et al. Mechanical failure of prosthetic human implants: a 10-year experience with aortic stent graft devices. *J Vasc Surg*. 2003;37:16–26.
7. Krajcer Z, Howell M, Dougherty K. Unusual case of AneuRx stent-graft failure two years after AAA exclusion. *J Endovasc Ther*. 2001;8: 465–471.

8. Dowdall JF, Greenberg RK, West K, et al. Separation of components in fenestrated and branched endovascular grafting--branch protection or a potentially new mode of failure? *Eur J Vasc Endovasc Surg*. 2008;36:2–9.
9. Zarins CK, Bloch DA, Crabtree T, et al. Stent graft migration after endovascular aneurysm repair: importance of proximal fixation. *J Vasc Surg*. 2003;38:1264–1272.
10. Beebe HG, Cronenwett JL, Katzen BT, et al. Results of an aortic endograft trial: impact of device failure beyond 12 months. *J Vasc Surg*. 2001;33:S55–63.
11. Abraham CZ, Chuter TA, Reilly LM, et al. Abdominal aortic aneurysm repair with the Zenith stent graft: short to midterm results. *J Vasc Surg*. 2002;36:217–225.
12. Abel DB, Beebe HG, Dedashtian MM, et al. Preclinical testing for aortic endovascular grafts: results of a Food and Drug Administration workshop. *J Vasc Surg*. 2002;35: 1022–1028.
13. Abel DB, Dehdashtian MM, Rodger ST, et al. Evolution and future of preclinical testing for endovascular grafts. *J Endovasc Ther*. 2006; 13:649–659.
14. Bargeron CB, Hutchins GM, Moore GW, et al. Distribution of the geometric parameters of human aortic bifurcations. *Arteriosclerosis*. 1986;6:109–113.
15. O'Flynn PM, O'Sullivan G, Pandit AS. Methods for three-dimensional geometric characterization of the arterial vasculature. *Ann Biomed Eng*. 2007;35:1368–1381.
16. Sternbergh WC, Money SR, Greenberg RK, et al. Influence of endograft oversizing on device migration, endoleak, aneurysm shrinkage, and aortic neck dilation: results from the Zenith Multicenter Trial. *J Vasc Surg*. 2004;39: 20–26.
17. Draney MT, Alley MT, Tang BT, et al. Importance of 3D nonlinear gradient corrections for quantitative analysis of 3D MR angiographic data. Paper presented at: International Society for Magnetic Resonance in Medicine; May 18-24, 2002; Honolulu, HI, USA.
18. Choi G, Cheng CP, Wilson NM, et al. Methods for quantifying three-dimensional deformation of arteries due to pulsatile and nonpulsatile forces: implications for the design of stents and stent grafts. *Ann Biomed Eng*. 2009;37:14–33.
19. Heikkinen MA, Alsac JM, Arko FR, et al. The importance of iliac fixation in prevention of stent graft migration. *J Vasc Surg*. 2006;43: 1130–1137.
20. Benharash P, Lee JT, Abilez OJ, et al. Iliac fixation inhibits migration of both suprarenal and infrarenal aortic endografts. *J Vasc Surg*. 2007;45:250–257.
21. Cheng CP, Choi G, Herfkens RJ, et al. The effect of aging on deformations of the superficial femoral artery due to hip and knee flexion: potential clinical implications. *J Vasc Interv Radiol*. 2009:In press.
22. Kadaba MP, Ramakrishnan HK, Wootten ME. Measurement of lower extremity kinematics during level walking. *J Orthop Res*. 1990;8: 383–392.